Quantum signatures of breathers in a finite Heisenberg spin chain

2010 J. Phys.: Condens. Matter 22 205502

(http://iopscience.iop.org/0953-8984/22/20/205502)

J. Phys.: Condens. Matter **22** (2010) 205502 (11pp) doi:10.1088/0953-8984/22/20/205502

Quantum signatures of breathers in a finite Heisenberg spin chain

Z I Djoufack[1,2], A Kenfack-Jiotsa[1,3], J P Nguenang[4,5] and S Domngang[2]

[1] Nonlinear Physics and Complex Systems Group, Département de Physique, Ecole Normale Supérieure, Université de Yaoundé I, PO Box 47, Yaoundé, Cameroon
[2] Materials Sciences Laboratory, Département de Physique, Faculté des Sciences, Université de Yaoundé I, PO Box 812, Yaoundé, Cameroon
[3] A S International Centre for Theoretical Physics, Strada Costiera 11, Trieste, Italy
[4] Fundamental Physics Laboratory, Group of Nonlinear Physics and Complex Systems, Department of Physics, Faculty of Sciences, University of Douala, PO Box 24157, Douala, Cameroon

E-mail: nguenang@yahoo.com

Received 28 October 2009, in final form 31 March 2010
Published 30 April 2010
Online at stacks.iop.org/JPhysCM/22/205502

Abstract
A map of a quantum Heisenberg spin chain into an extended Bose–Hubbard-like Hamiltonian is set up. Within this framework, the spectrum of the corresponding Bose–Hubbard chain, on a periodic one-dimensional lattice containing two, four, and six bosons shows interesting detailed band structures. These fine structures are studied using numerical diagonalization, and nondegenerate and degenerate perturbation theory. We also focus our attention on the effect of the anisotropy and Heisenberg exchange energy on the detailed band structures. The signature of the quantum breather is also set up by the square of the amplitudes of the corresponding eigenvectors in real space.

(Some figures in this article are in colour only in the electronic version)

1. Introduction

The phenomenon of localization and transport of energy in discrete lattices by discrete breathers has received considerable attention in recent years both from the theoretical and experimental points of view [1–3]. These excitations are generic time-periodic and spatially localized solutions of the underlying classical Hamiltonian lattice with translational invariance. Their spatial profiles localize exponentially for short-range interactions. Recently, the application of these ideas to the normal mode space has allowed us to explain some facets of the Fermi–Pasta–Ulam (FPU) paradox [4–8]. The problem consists of the nonequipartition of energy among normal modes of a weakly anharmonic atomic model. In the harmonic limit, each normal mode corresponds to a periodic orbit in phase space and is characterized by its wavenumber q. Such an investigation of localized excitations in normal mode space from the harmonic limit into the FPU parameter regime allows us to realize the persistence of periodic orbits, termed q-breathers. In the normal mode space, although the interaction is long ranged, it is selective and purely nonlinear, thus q-breathers localize exponentially for classical investigations.

Before using quantum breathers, it is important to specify the correct correspondence relation between a classical model and its quantum mechanical counterpart [9]. Quantum breathers consist of superpositions of nearly degenerate many-quanta bound states, with very long times to tunnel from one lattice site to another [10]. These quantum excitations although being extended states in a translationally invariant system are characterized by exponentially localized weight functions, in full analogy to their classical counterparts.

Studies of quantum modes on small lattice are of interest for quantum devices based on quantum dots, for studies of photonic crystals, Josephson junction arrays [11], arrays of weakly coupled waveguides, protein-like crystals [12], and possibly in myoglobin [13], for the studies of Bose–Einstein condensates in periodic optical traps [14], light propagation in interacting optical waveguides, and cantilever vibrations

[5] Author to whom any correspondence should be addressed.

in micromechanical arrays. It has also been shown that the intrinsic localized modes can occur in isotropic ferromagnetic chains [15]. In many cases, quantum dynamics is important.

It is worth mentioning that recent experimental investigations show that we can observe quantum breathers in coupled Josephson junctions. In this specific system, Pinto and Flach [16] found that the presence of the anharmonicity in the potential of two capacitively coupled Josephson junctions allows localization of quantum excitations that henceforth localize energy on one junction during a time that sensitively depends on their energy. They can be tuned through the bias current injected into the junctions' manipulation techniques that nowadays are used for quantum information processing with Josephson junctions. Such a system can be used to resolve the flow of energy between the junctions in time.

Discrete breathers are nonlinear localized modes that can be created in translationally invariant nonlinear lattice models. They can modify the system's properties such as the thermodynamics of the lattice and introduce the possibility of nondispersive energy during its transport. Investigations of discrete breathers or intrinsic localized modes in recent years has revealed a wealth of new properties of energy localization. Relaxation and mobility, in particular, may have critical links with biomolecular processes [17]. The study of the spectrum and eigenstates of the quantum breathers is less known for the case of systems containing more than two bosons. Indeed there are several published papers for the case of two bosons. For instance, Nguenang *et al* [18] investigated the localization properties of the eigenstates in a finite Bose–Hubbard chain and they observed localization of the weight function as a function of the wavenumber, which they interpret as a signature of quantum q-breather excitations displaying an algebraic decay, at variance with the exponential decay of the q-breathers in the case of a classical nonlinear system [18]. Two-vibron bound states have been investigated in the β-Fermi–Pasta–Ulam model [19] as well as in [9, 20–29]. The most extensively studied system is the discrete nonlinear Schrödinger equation with two particles (a dimer). This system is integrable due to the existence of two integrals of motion (energy and boson number). The classical version can be completely solved. Bernstein *et al* [31, 32] and Aubry *et al* [32] studied the expected splitting of degenerate pairs of eigenvalues in the quantum system. In practice, less is known for systems with many degrees of freedom. It is only Dorignac *et al* [8, 23] and Eilbeck [33] who have studied the spectrum of the quantum discrete nonlinear Schrödinger equation, in the case of four and six bosons using degenerate perturbation theory. The output suggested exponentially small band widths for quantum breather bands with large boson number [9, 30, 34]. However, in the case of a Heisenberg spin system very few studies have been mostly devoted to classical discrete breathers within the modulational instability framework [15, 35]. From the foregoing it is clear that the study of the localization of energy in a quantum Heisenberg spin chain is less investigated and needs a detailed inspection.

In this paper, we investigate the spectrum of an extended Bose–Hubbard-like lattice derived from a specific map of a one-dimensional (1D) Heisenberg spin system. One important point about the localization is the question of knowing how localized the excitations in such a physical are. The first step to answer such a question is to probe the energy band of the system under consideration. From such an investigation, important an new features can be determined. Using a numerical diagonalization of the so-derived Hamiltonian, nondegenerate and degenerate perturbation theory, we study the spectrum of the two, four, and six bosons for the quantum Heisenberg spin chain within the mapping scheme. In section 2, we describe the model. In section 3, we introduce the basis used to write down the Hamiltonian matrix then we derive the analytical expression of the eigenvalue spectrum. In section 4, we study the influence of exchange interaction and anisotropy interaction on the eigenvalue spectrum in a periodic lattice containing two bosons. In section 5, we present the numerical results by using the diagonalization of the Hamiltonian matrix to derive the energy spectrum for four and six bosons. In section 6, we conclude our study.

2. Model Hamiltonian and the mapping

We use a model for the classical Heisenberg ferromagnetic spin chain.

$$H_1 = -\sum_i J\vec{S}_i \cdot \vec{S}_{i+1}. \tag{1}$$

Here, $\vec{S}_i = (S_i^x, S_i^y, S_i^z)$ is the spin angular momentum vector, J is the exchange interaction parameter. We introduce the classical quantity $S_c = \hbar S$ and a condition which allows the transformation of equation (1) into a quantum spin system. We also introduce a dimensionless spin variable $\hat{S}_i = \frac{\vec{S}_i}{\hbar}$ and define $\hat{S}_i^{\pm} = \hat{S}_i^x \pm \mathrm{i}\hat{S}_i^y$. We recast the Hamiltonian into the following dimensionless form

$$\hat{H}_1 = -\sum_i \frac{J}{2}[\hat{S}_i^+\hat{S}_{i+1}^- + \hat{S}_i^-\hat{S}_{i+1}^+ + 2\hat{S}_i^z\hat{S}_{i+1}^z]. \tag{2}$$

It is impossible to diagonalize the Hamiltonian (2) by a canonical transformation, but it is possible to transform it to the new dimensionless one, using either pure Bose or pure Fermi operators [36, 37]. $\hat{S}_i$ satisfies the commutation relations $[\hat{S}_i^+, \hat{S}_j^-] = 2\hat{S}_i^z\delta_{ij}$, $[\hat{S}_i^{\pm}, \hat{S}_j^z] = \pm\hat{S}_i^{\pm}\delta_{ij}$, with $\hat{S}_i \cdot \hat{S}_i = S(S+1)$. In this respect, the Hamiltonian maintains a relatively simple form. To this end, we use the Holstein–Primakoff transformation [38] for the local spin operators to treat the system from the semi-classical approach as compared to the quantum version in terms of bosonic creation and annihilation operators as

$$\begin{aligned}\hat{S}_i^+ &= \sqrt{2}[1-\epsilon^2 a_i^\dagger a_i]^{1/2}\epsilon a_i\\ \hat{S}_i^- &= \sqrt{2}\epsilon a_i^\dagger[1-\epsilon^2 a_i^\dagger a_i]^{1/2}\\ \hat{S}_i^z &= [1-\epsilon^2 a_i^\dagger a_i],\end{aligned} \tag{3}$$

where $\epsilon = \frac{1}{\sqrt{S}}$. Using equations (3), a quantum Hamiltonian can be obtained in a power series of ϵ, which is rescaled by $J\epsilon^2$ as a sum of

$$\hat{H}_{10} = -\sum_i^f [a_i^\dagger a_{i+1} + a_i a_{i+1}^\dagger - (a_i^\dagger a_i + a_{i+1}^\dagger a_{i+1})] \tag{4}$$

and

$$\hat{H}_{11} = \tfrac{1}{4}\sum_{i}^{f}[a_i^\dagger a_i^\dagger a_i a_{i+1} + a_i^\dagger a_{i+1}^\dagger a_{i+1} a_{i+1} + a_i^\dagger a_i a_i a_{i+1}^\dagger + a_i a_{i+1}^\dagger a_{i+1}^\dagger a_{i+1} a_{i+1} + 2a_i^\dagger a_i a_{i+1}^\dagger a_{i+1}] \quad (5)$$

f is the number of sites in a 1D periodic lattice, $a_i^\dagger$ and a_i being the bosonic creation and annihilation operators respectively, satisfying the usual commutation relations $[a_i, a_j^\dagger] = \delta_{ij}$, $[a_i^\dagger, a_j^\dagger] = 0$ and $[a_i, a_j] = 0$. In this way, the total Hamiltonian of the system can be written as the sum of two terms.

$$\hat{H}_1 = \hat{H}_{10} + \gamma \hat{H}_{11} \quad (6)$$

where $\gamma = \epsilon^2$ is the parameter controlling the strength of the interaction.

3. Energy spectrum for the two-boson state in the model

To describe the components of the quantum states, we use a position state representation $|\psi_i\rangle = |n_1, n_2, \ldots, n_f\rangle$, where n_i represents the number of bosons at site i ($n = \sum_i n_i$). For example, the state $|11000\cdots0\rangle$ represents a state with one boson at the site 1, another boson at site 2, and nothing elsewhere.

Considering the fact that the chain of length f is subject to periodic boundary conditions, we can apply the translation operator to these states. The chain is translationally invariant and the Hamiltonian of this quantum system commutes with the number operator $\hat{N} = \sum_{i=1}^{f} a_i^\dagger a_i$, whose eigenvalue is n. For a given number of bosons, each eigenstate is a linear combination of the number state with fixed n. In addition to the number of quanta n, there are $n-1$ further quantum numbers which define the relative distance between the bosons.

For the sake of simplicity, we consider an odd number of sites $f = 2\sigma + 1$, where σ can take $\frac{f+1}{2}$ different values. A general eigenfunction of these states for the Hamiltonian (6) is a Bloch wave that can be written as (see the notation in [1, 8, 9, 18, 20])

$$|\psi\rangle = \sum_{i=1}^{\sigma} C_i |\psi_i\rangle. \quad (7)$$

We can construct the number states that are also Bloch states as

$$|\psi_i\rangle = \frac{1}{\sqrt{f}} \sum_{s=1}^{f} \left(\frac{\hat{T}}{\tau}\right)^{s-1} \Big|1\underbrace{0\cdots0}_{i-1}1\Big\rangle. \quad (8)$$

Here $\hat{T}$ is the translation operator and $k = 2\pi\nu/f$, with $\nu \in \{-\frac{f+1}{2}, \frac{f-1}{2}\}$ and $\tau = \mathrm{e}^{ik}$ being the eigenvalue of the translational operator $\hat{T}$. To ensure that $\langle\psi|\psi\rangle = 1$, it is necessary that $C_1, C_2, \ldots$ are normalized as $\sum_{i=1}^{(f+1)/2} |C_i|^2 = 1$. The lattice under consideration is a homogeneous quantum lattice with periodic boundary conditions. Therefore it is possible to block diagonalize the Hamiltonian operator using eigenfunctions of the translation operator $\hat{T}$ defined as $\hat{T} a_i^\dagger = a_{i+1}^\dagger \hat{T}$, so that $\hat{T}[n_1, n_2, \ldots, n_f] = [n_f, n_1, \ldots, n_{f-1}]$. In each block, the eigenfunctions have a fixed value of the momentum k [19]. With the basis introduced in equation (8), we can derive the matrix elements after introducing the dimensionless Hamiltonian using $\widetilde{H_{kl}} = \langle\psi_k|\tilde{H}|\psi_l\rangle$. We obtain the Hamiltonian matrix in the following equation

$$\tilde{H}_1 = \frac{\hat{H}_1}{J} = -\begin{pmatrix} u & \sqrt{2}q & \cdots & & & \\ \sqrt{2}q^* & y & g & & & \\ & g^* & u & g & & \\ \vdots & & \ddots & \ddots & \ddots & \\ & & & g^* & u & g \\ & & & & g^* & P \end{pmatrix}, \quad (9)$$

where $P = \tau^{-\frac{f+1}{2}} + \tau^{-\frac{f-1}{2}} + u$, $u = -4$, $y = u + \gamma/2$, $q = (\frac{\gamma}{4} - 1)g$, and $g = 1 + \tau$.

The structure of the Hamiltonian matrix obtained in equation (9) is similar to the two-bosons case described in [10, 16–21, 24, 33] and the four-bosons case described in [8]. We can derive the eigenenergies for each given Bloch wavenumber k from the Schrödinger equation given by $\hat{H}|\psi_k\rangle = E|\psi_k\rangle$.

Using numerical diagonalization as in [20, 36, 37], we can derive the eigenvalue spectrum of the corresponding Heisenberg spin chain. We have plotted numerically the energy spectrum as a function of wavenumber k for the interaction strength $\gamma = 1$.

This is shown in figure 1(a), where the result are obtained from the numerical diagonalization of the Hamiltonian matrix (9). Here, it is clear that an isolated ground-state eigenvalue appears for each k that corresponds to a bound state [18, 20, 22]. For this isolated ground state, there is a high probability of finding two quanta on the same site. Similar phenomena have been obtained in other nonlinear models in [8] for the case of four particles and in [18–20, 22, 25–28, 40–42] for two particles. Figure 1 clearly shows the energy spectrum composed essentially of a localized band below the delocalized band.

We have shown in figure 1(b) the square wave amplitudes of the corresponding eigenvectors in real space for a localized state. From a physical picture of a ferromagnetic spin chain, the continuum band here is describing a magnetic spin chain with completely delocalized excitation along the chain whereas the case of a single band for two on-site bosons corresponds to the case of only one spin that can be excited by two switches. Figure 1(b) shows that the wavefunction is localized and indicates that there is a high probability of finding two bosons on the same sites.

4. Effect of the exchange and anisotropy interaction on the two-boson state energy's spectrum

We describe the novel Hamiltonian for an anisotropic ferromagnetic chain. The corresponding Heisenberg Hamiltonian can be written as

$$H_2 = H_1 + \sum_i A(S_i^z)^2. \quad (10)$$

The term proportional to A represents the single-ion uniaxial anisotropy due to crystal field effect and A is the anisotropy

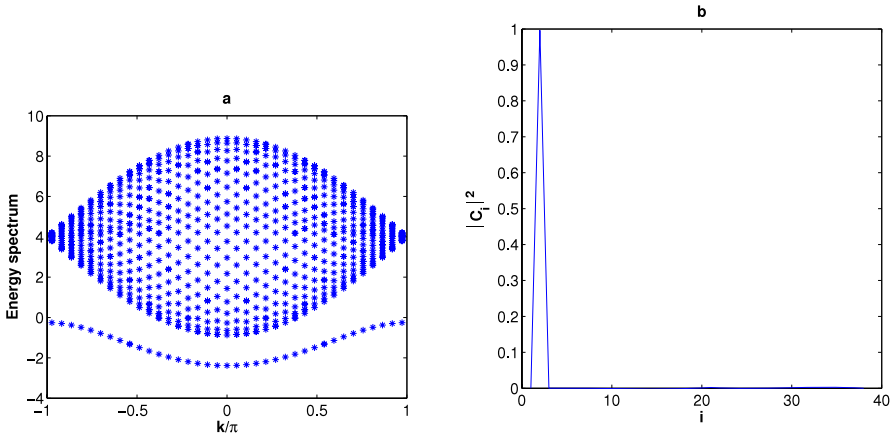

Figure 1. (a) Energy spectrum of the two bosons in the extended Bose–Hubbard chain; (b) square wave amplitudes of the eigenvectors in real space. Here the value of the interaction strength $\gamma = 1$, $n = 2$, and $f = 37$.

parameter. If the anisotropy parameter $A < 0$, the system is associated with an easy axis spin chain and if $A > 0$, the spin system is said to have an easy plane anisotropy for the spin chain. We can derive the discrete quantum Hamiltonian using Holstein–Primakoff bosonic representation, then equation (10) can be written after introducing dimensionless Hamiltonian

$$\hat{H}_2 = \hat{H}_{20} + \gamma \hat{H}_{21} + O(\gamma^2). \tag{11}$$

Hence we set

$$\hat{H}_{20} = \hat{H}_{10} + 2\frac{A}{J}\sum_{i}^{f} a_i^{\dagger} a_i \tag{12}$$

and

$$\hat{H}_{21} = \hat{H}_{11} - 4\frac{A}{J}\sum_{i}^{f} a_i^{\dagger} a_i a_i^{\dagger} a_i. \tag{13}$$

We also use the basis introduced in equation (8) to calculate the matrix elements for a dimensionless Hamiltonian. In this way the Hamiltonian matrix can be written as

$$\tilde{H} = \frac{\hat{H}}{J} = -\begin{pmatrix} t & \sqrt{2}q & & \cdots & & \\ \sqrt{2}q^* & t+\gamma/2 & g & & & \\ & g^* & t & g & & \\ \vdots & & \ddots & \ddots & \ddots & \\ & & & g^* & t & g \\ & & & & g^* & P \end{pmatrix}, \tag{14}$$

where $P = \tau^{-\frac{f+1}{2}} + \tau^{-\frac{f-1}{2}} + t$, $q = (\frac{\gamma}{4} - 1)g$, $t = -4[1 + \frac{A}{J}(1-\gamma)]$, $g = 1 + \tau$.

The structure of the Hamiltonian matrix obtained in equation (14) is similar to two-vibron bound states in the β-Fermi–Pasta–Ulam model described in [19].

Now let us use a numerical diagonalization to derived the eigenvalue spectrum for the anisotropic ferromagnetic chain and probe the influence of the exchange interaction on the energy spectrum.

In this respect we introduce as an example the following set of parameters of the $CsNiF_3$ material which is a best example of 1D spin system, namely $J = 23.6$ and $A = 9$. For this case, the energy spectrum is composed also by the continuum band above the single band, as illustrated in figures 2(a) and (b).

Modifying the parameters of the $CsNiF_3$ material is also supported by the idea that such a material may also face some physical constraints such as heating or magnetostriction effects that can lead to the modification of its physical parameters. For the ferromagnetic materials' case, characterized by $J = 23.6$ and $A > 9$, the energy spectrum for these materials is always composed of the continuum band above the single band. Here we notice that, with increasing the anisotropy parameter of the material the single band progressively merges into the continuum band and the complete merging of the single band into the continuum occurs for the anisotropy parameter $A = 48$. This is clearly shown in figure 2(c). It is also realized that keeping this value of the exchange integral parameter in the range $J = 23.6$ and then increasing the anisotropy parameter to $A = 70$, the single band can appear above the continuum, as seen in figure 2(d).

From these later figures, we notice that when the exchange interaction is constant, increasing the anisotropy parameter contributes to modifying the localized states.

In the case of ferromagnetic materials with $J = 23.6$ and $A < 9$, the continuum band does not merge the single band, the width of the gap progressively increases when the anisotropy parameter's value decreases. However, for $A \leqslant 0.01$ the width of the gap becomes constant.

We also noticed that for ferromagnetic materials where $J > 23.6$ and $A > 9$, their energy spectrum is comparable to the case of a ferromagnet with $J = 23.6$ and $A < 9$, displaying a gap with constant width.

Needless to mention is the fact that, for the ferromagnetic materials with $J < 23.6$ and $A = 9$, it is realized that as the exchange integral parameter is decreasing, the gap between the continuum and the single band reduces so that a complete merging of the single band into the continuum band occurs for $J = 4$ and $A = 9$, such as the case seen in figure 2(c). When the exchange integral $J < 4$, it is realized that the single band changes its concavity initially below and takes a reverse concavity above the continuum. The continuum band leaves

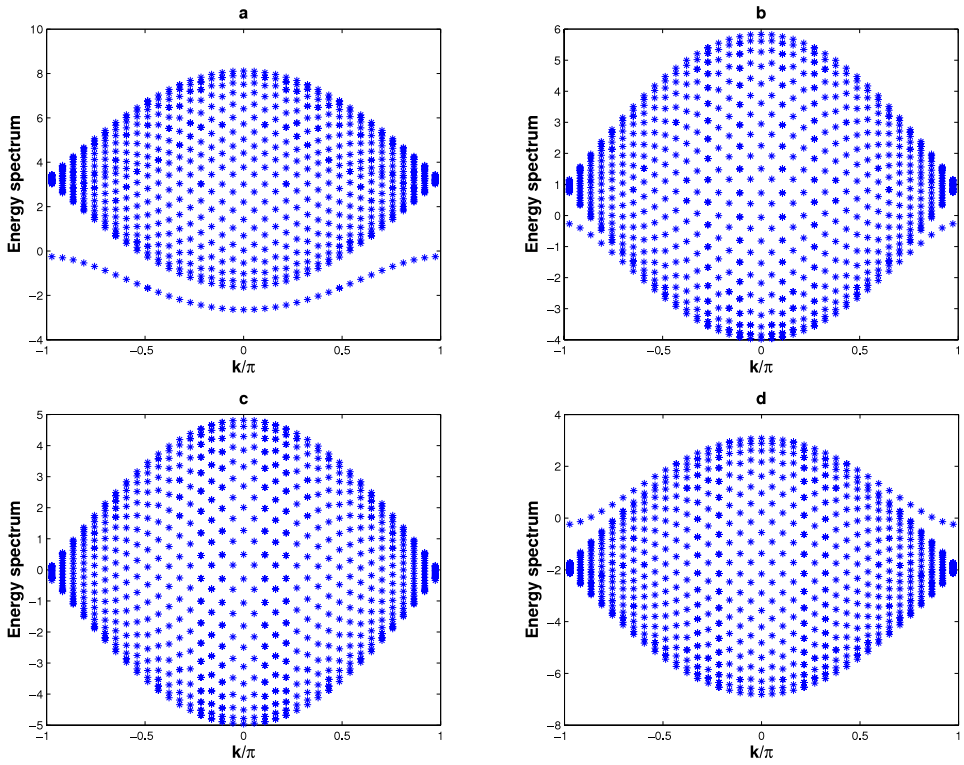

Figure 2. Energy spectrum of the two bosons in the extended Bose–Hubbard chain for different values of exchange interaction and anisotropy parameter where the value of the interaction strength is $\gamma = 1$, $n = 2$, and $f = 37$: (a) $J = 23.6$ and $A = 9$, (b) $J = 23.6$ and $A = 36$, (c) $J = 23.6$ and $A = 48$, (d) $J = 23.6$ and $A = 70$.

the single band and the width of the gap becomes larger when J decreases. This phenomenon is depicted in figures 3(a)–(c).

Here we also notice that the width of the gap progressively increases as the exchange integral J decreases. On varying the values of the exchange interaction parameter, some little difference in the spectrum occurs just as a matter of ordering the position of the bands in the energy spectrum.

To probe the existence probability of a given localized state for the corresponding ferromagnetic chain, we also plotted the square of the eigenvectors in real space for different values of anisotropy and exchange interaction. As a result we obtained the same figures as those plotted previously in figure 1(b), from a physical picture applied to magnetic material in the framework of a spin system it is important to mention the fact that there is a limitation i.e. $n \leqslant 2S$. In the case of $CsNiF_3$ material $S = 1$ and since the localized states occur for $n = 2$ the bound states occurring in figures 1 and 2 are the result of a localized states constituted of two adjacent spins engaged in a switching process. This process is revealing an intrinsic local magnetization process that occurs in such a ferromagnet.

5. Energy spectrum for the four or six bosons in the extended Bose–Hubbard chain

In this section we consider the same Hamiltonian given in equation (10) with rescaling at ϵ^2. Before using degenerated perturbation theory, it is important to know that all bosons on the same band might have the same energy. The Hamiltonian of equation (10) shows that all bosons on the same band have different energy at zero anisotropy coupling ($A = 0$). In order to discourage many bosons from occupying the same site, we can derived a Bose–Hubbard-like lattice from a specific anisotropic term by using the usual commutation relations of the bosonic operators. For this we start by defining the perturbed Hamiltonian as $\hat{H} = \hat{H}_0 + \hat{V}$, where $\hat{H}_0$ is the nonlinear on-site interaction Hamiltonian given by

$$\hat{H}_0 = \sum_i^f A\gamma a_i^\dagger a_i^\dagger a_i a_i. \tag{15}$$

If $A < 0$, the model is also known to describe an attractive interaction or a repulsive one if $A > 0$. All the other terms of the Hamiltonian describe the nonlinear interaction within the particles located in adjacent sites, including the hopping term and linear on-site interaction terms. This is denoted by $\hat{V}$.

$$\begin{aligned}\hat{V} = -\sum_i^f \Big(& J[a_i^\dagger a_{i+1} + a_i a_{i+1}^\dagger - (a_i^\dagger a_i + a_{i+1}^\dagger a_{i+1})] \\ & + A(a_i^\dagger a_i) + \frac{\gamma}{4} J[(a_i^\dagger a_i^\dagger a_i a_{i+1} + a_i^\dagger a_{i+1}^\dagger a_{i+1} a_{i+1}) \\ & + (a_i^\dagger a_i a_i a_{i+1}^\dagger + a_i a_{i+1}^\dagger a_{i+1}^\dagger a_{i+1}) + 2a_i^\dagger a_i a_{i+1}^\dagger a_{i+1}]\Big).\end{aligned} \tag{16}$$

To describe the components of the quantum states, we use a position state basis representation as in section 3. For instance, the state $|\psi_i\rangle = |2000110\rangle$ represents a state with two bosons

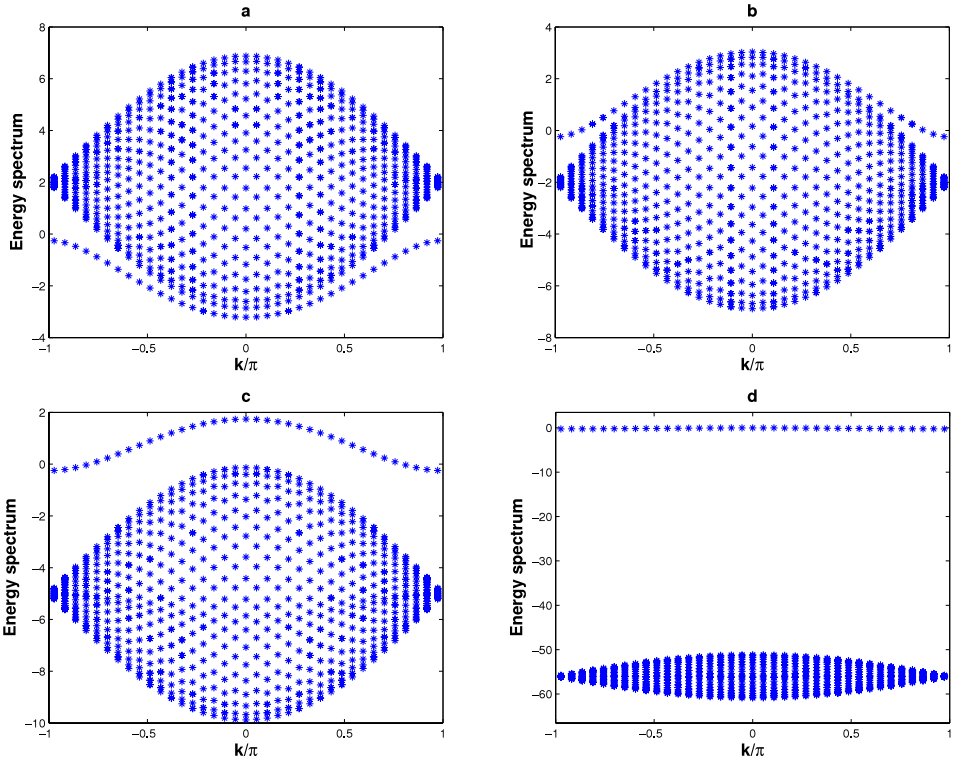

Figure 3. Energy spectrum of the two bosons in the extended Bose–Hubbard chain for different values of exchange integral parameter where the value of the interaction strength is $\gamma = 1$, $n = 2$, and $f = 37$: (a) $J = 9$ and $A = 9$, (b) $J = 2$ and $A = 9$, (c) $J = 2$ and $A = 9$, (d) $J = 0.5$ and $A = 9$.

at site 1, one boson at site 5, one boson at site 6 and no bosons elsewhere. In view of the periodic structure of the lattice, the chain is translationally invariant and the Hamiltonian of this quantum system commutes with the number operator $\hat{N} = \sum_{i=1}^{f} a_i^{\dagger} a_i$, whose eigenvalue is denoted by n. We can generate an equivalence class of states by applying the translation operator with periodic boundary conditions to one of these states. We can manage to order these classes. For example, the set of all classes containing $|22\rangle$, $|202\rangle$, $|2002\rangle$, and so on, is referred to as the $\{2, 2\}$ band. All classes containing $|42\rangle$, $|402\rangle$, $|4002\rangle$, ... are referred to as the $\{4, 2\}$ band. All the classes containing $|24\rangle$, $|204\rangle$, $|2004\rangle$, ... are referred to as the $\{2, 4\}$ band and all the classes containing $|33\rangle$, $|303\rangle$, $|3003\rangle$, ... are referred to as $\{3, 3\}$ bands.

Bands involving the interaction of single bosons with composite states, such as $\{2, 1, 1\}$, $\{3, 1\}$, $\{4, 1, 1\}$, $\{3, 1, 1, 1\}$, $\{5, 1\}$, $\{1, 1, 2\}$, $\{1, 3\}$, $\{1, 1, 4\}$, $\{1, 1, 1, 3\}$, $\{1, 5\}$, ..., are more difficult to analyze and do not reveal interesting structures. Hence, we do not consider these bands in the present study provided that the main information is not lost. This section is devoted to the fine structure of the $\{2, 2\}$, $\{4, 2\}$, $\{2, 4\}$, and $\{3, 3\}$ bands.

If the anisotropy is considered without the Hamiltonian term denoted by $\hat{V}$, the states $|22\rangle$, $|202\rangle$, $|2002\rangle$, ..., of all previously mentioned bands are degenerate. Therefore, we use degenerated perturbation theory to obtain both eigenvalues and eigenvectors for the case of the perturbed Hamiltonian. For a given number of bosons, each eigenstate is a linear combination of the number of states with fixed n. In addition to the number of quanta n, there are $n - 1$ further relative distances $i - 1$ between the four and six quanta. We consider an odd number of sites $f = 2\sigma + 1$, which can take $(f + 1)/2$ different values for the sake of simplicity. We do proceed in the same way as in section 3, then the Bloch waves of $\{2, 2\}$, $\{4, 2\}$, $\{2, 4\}$, and $\{3, 3\}$ states can be written in the notation of [18, 20, 37] as

$$|\psi\rangle = \sum_{j=1}^{\sigma} C_i |\psi_i\rangle, \qquad \sigma = \frac{f-1}{2}. \tag{17}$$

We can construct number states with Bloch waves as

$$\begin{aligned}
|\psi_i\rangle &= \frac{1}{\sqrt{f}} \sum_{s=1}^{f} \left(\frac{\hat{T}}{\tau}\right)^{s-1} \Big|2\underbrace{0\cdots0}_{i-1}2\Big\rangle \\
|\psi_i\rangle &= \frac{1}{\sqrt{f}} \sum_{s=1}^{f} \left(\frac{\hat{T}}{\tau}\right)^{s-1} \Big|4\underbrace{0\cdots0}_{i-1}2\Big\rangle \\
|\psi_i\rangle &= \frac{1}{\sqrt{f}} \sum_{s=1}^{f} \left(\frac{\hat{T}}{\tau}\right)^{s-1} \Big|2\underbrace{0\cdots0}_{i-1}4\Big\rangle \\
|\psi_i\rangle &= \frac{1}{\sqrt{f}} \sum_{s=1}^{f} \left(\frac{\hat{T}}{\tau}\right)^{s-1} \Big|3\underbrace{0\cdots0}_{i-1}3\Big\rangle.
\end{aligned} \tag{18}$$

Here $\hat{T}$ is the translation operator and $\tau = \mathrm{e}^{\mathrm{i}k}$, with $k = 2\pi\nu/f$ and $\nu \in \{-\sigma, \ldots, \sigma\}$. Using standard Brillouin–Wigner

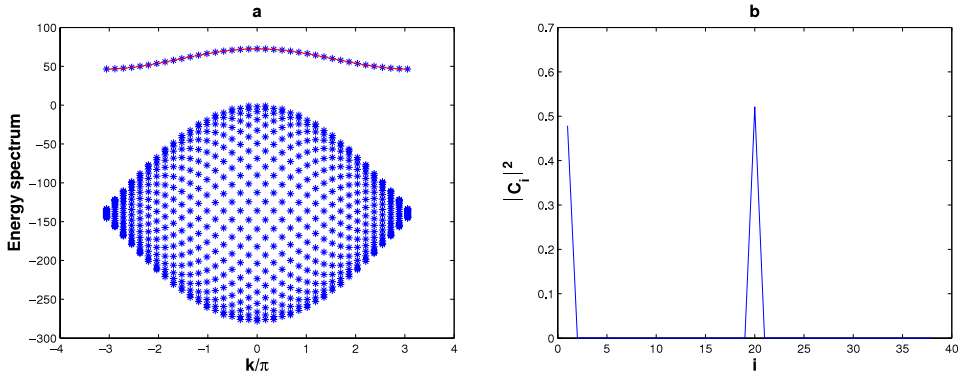

Figure 4. (a) Detail of the energy spectrum for the Bose–Hubbard model derived from the anisotropic Heisenberg model in a periodic lattice where $n = 4$, $f = 37$, $J = 22$, and $\gamma = 0.25$: (a) repulsive for $A = 7$; (b) square of the wavefunction amplitudes corresponding to the eigenvectors as a function of the position of the band along the chain.

perturbation to the second order approximation, we define the Hamiltonian matrix element as (in the notation of [7])

$$H_{i,i'}^{(m,l)} = \sum_{\tilde{\psi}} \frac{\langle\psi_i|V|\tilde{\psi}\rangle\langle\tilde{\psi}|V|\psi_{i'}\rangle}{E^{(0)} - \tilde{E}^{(0)}} \tag{19}$$

where $|\tilde{\psi}\rangle$ is any state not in the $\{2, 2\}$, $\{4, 2\}$, $\{2, 4\}$, and $\{3, 3\}$ subspace; $\tilde{E}^{(0)}$ is the corresponding energy of $|\tilde{\psi}\rangle$ while $E^{(0)}$ is the energy of (m, l) bosons on the same site at zero coupling. The expression of this energy is given as

$$E_l^{(0)} = A\gamma l(l-1). \tag{20}$$

We can use equation (20) to evaluate the energy of l bosons on the same site. For instance, in the case of $n = 4$, the $\{4\}$ band has energy $E_4^{(0)} = 12A\gamma$, the $\{3, 1\}$ band has energy $E_3^{(0)} = 6A\gamma$, the $\{2, 1, 1\}$ band has energy $E_2^{(0)} = 2A\gamma$, the $\{2, 2\}$ band has energy $2E_2^{(0)} = 4A\gamma$, and so on.

Considering the lattice with four bosons ($n = 4$). We can subdivide this case into several bands. The lowest band is a linear combination of states with four bosons on a given site i and no bosons elsewhere. The next lowest band is composed of states with three bosons on site and another boson elsewhere. The third band consists of states with two bosons on one site and two bosons on a separate site. Bands involving the interactions of single bosons with composite states, such as $\{3, 1\}$, $\{1, 3\}$, $\{1, 1, 2\}$, and $\{1, 1, 2\}$ are not considered here because they are more difficult to analyze. We consider here only the $\{2, 2\}$ band because it presents great interest since it represents the simplest case of a band describing two particles interacting with each other. Using the previous formulation given by equations (19) and (20), we obtain the $\{2, 2\}$ band Hamiltonian matrix as

$$H^{(2,2)} = -\frac{4J^2B}{A\gamma} I_\sigma - \frac{J^2B}{A\gamma} \begin{pmatrix} \Gamma & W & & & \\ W^* & 0 & W & & \\ & \ddots & \ddots & \ddots & \\ & & W^* & 0 & W \\ & & & W^* & P \end{pmatrix}, \tag{21}$$

where $B = (\frac{\gamma}{4} - 1)^2$, I_σ is the $\sigma \times \sigma$ unity matrix, $W = 1 + \tau = 2e^{ik/2}\cos(k/2)$, $P = 2\cos(\sigma k)$, $\Gamma = 6(\frac{C}{B} - 1)$, $C = (\frac{3\gamma}{4} - 1)^2$, and A is always the anisotropy parameter.

The structure of the matrix in equation (21) is very similar to the four-boson case described in [8] and the two-boson case described in [1, 18, 20]. Exact results can be obtained in the limit when the number of sites tends to infinity. In the limit $f \to \infty$,

$$E(k) = -\frac{3}{2}\frac{J^2B}{A\gamma} - \frac{J^2B}{A\gamma}\left(4 + \Gamma + \frac{4\cos^2(k/2)}{\Gamma}\right) \quad \text{if } |\Gamma| > 2\cos(k/2). \tag{22}$$

Using the same technique we have plotted the energy spectrum of a given material whose parameters are close to those of the $CsNiF_3$ structure with few bosons but with a different value of γ according to the limitation given by $n \leqslant 2S$.

The energy spectrum of the Hamiltonian matrix (21) is obtained by a numerical diagonalization method. The sign of the anisotropy parameter here determines whether the underlying Bose–Hubbard model is repulsive ($A > 0$), as shown by figure 4(a), or not. The fine structure of the ferromagnetic materials in the $\{2, 2\}$ band is constituted by a continuum band in addition to an isolated band and represents the ground state of a system with four bosons. The isolated band that appears either above or below the continuum is composed of states consisting of adjacent sites that are each occupied by two quanta. In the continuum band most of the sites are separated by one or more vacant sites. The localized band clearly describes the localization of energy that corresponds to the breather solution of the classical nonlinear system. This is the so-called soliton band [39, 40]. The stars correspond to the energy spectrum obtained from an exact numerical diagonalization of the matrix (21). For the case of the breather band, the lines represent its plot from the analytical equation (22) obtained in the limit when the number of sites tends to infinity. In the attractive case, the ground state is a localized state, located on two different positions along the chain illustrated by figure 4(b). This also illustrates the fact that there is a high probability of finding four bosons in two adjacent sites, each containing two bosons. It also represents the intrinsic localized mode with a complex character that the chain allows us to appreciate while plotting the eigenvector as a function of the position of particles. From a physical picture referred to the spin system, we shall

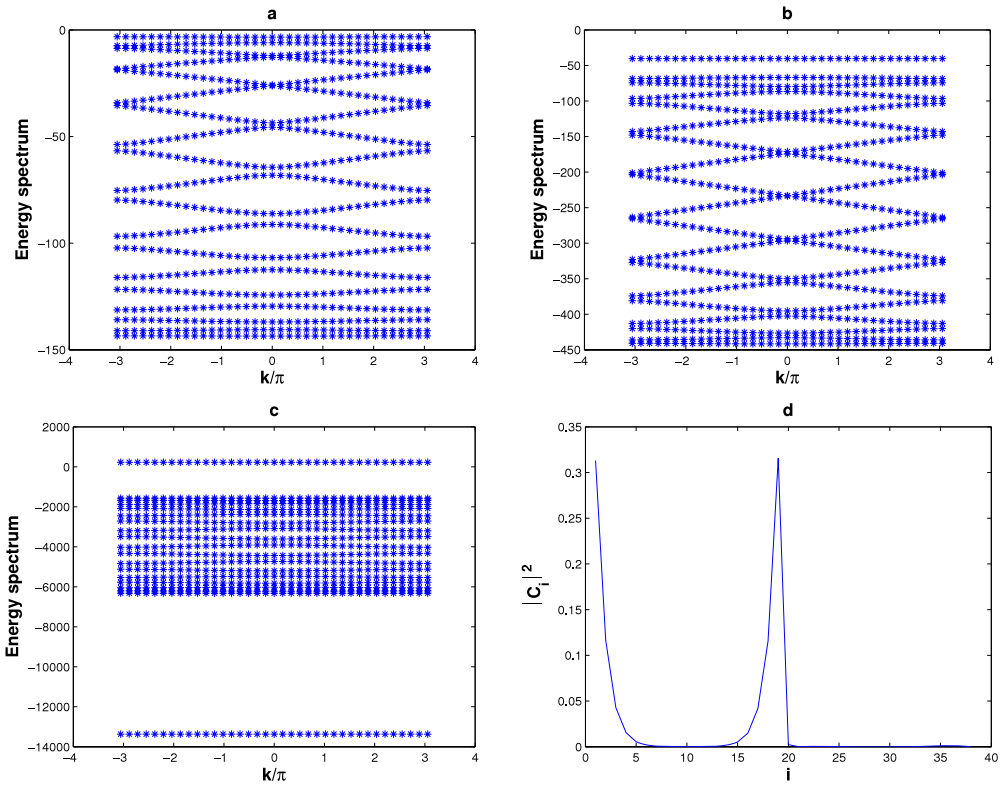

Figure 5. Detail of the energy spectrum for the extended Bose–Hubbard model, here $n = 6$, $f = 37$, and $\gamma = 0.5$: (a) case of repulsive nonlinearity where $A = 8$ and $J = 20$, $\gamma = 0.25$; (b) case of repulsive nonlinearity where $A = 9$ and $J = 16$; (c) case of repulsive nonlinearity where $A = 9$; $J = 26$ and $\gamma = 0.17$; (d) square wavefunction amplitudes.

keep in mind that the limitation given by $n \leqslant 2S$ allows only material with sufficiently high spin in order to display such a localization phenomenon that would lead a localized magnetization reversal process involving two group of two spins each.

Next, we consider the case of $n = 6$ bosons. This case displays three bands: namely the bands $\{4, 2\}$, $\{2, 4\}$, and $\{3, 3\}$.

In this case, the first band under consideration is the $\{4, 2\}$ band. Then if we proceed as in the case of the $\{2, 2\}$ band, it turns out that we obtain a Hamiltonian matrix describing this $\{4, 2\}$ band as

$$H^{(4,2)} = -\frac{2J^2}{3A\gamma}(3B + 2C)I_\sigma - \frac{BJ^2}{A\gamma}\begin{pmatrix} \Gamma & 1 & & & P^* \\ 1 & 0 & 1 & & \\ & \ddots & \ddots & \ddots & \\ & & 1 & 0 & 1 \\ P & & & 1 & \Gamma \end{pmatrix} \tag{23}$$

where $P = 6e^{ik\frac{D}{B}}$, $B = (\frac{\gamma}{4} - 1)^2$, $C = (\frac{3\gamma}{4} - 1)^2$, $D = (\frac{5\gamma}{4} - 1)^2$, and $\Gamma = -\frac{1}{3B}(3B + 2C - 13D)$.

The structure of the matrix in equation (23) is also a three diagonal matrix, which is different from the previous matrix in the position of their elements and very similar to the case of the six bosons described in [8]. The energies of this band do not depend on the crystal momentum k.

To characterize the energy spectrum of this band, we have also used parameters different from those of the $CsNiF_3$ structure.

The structure of the energy spectrum of these ferromagnetic materials is different from the $\{2, 2\}$ band by the rectangular form of the continuum band and is always composed of two bands where the single band can appear above for repulsive nonlinearity presented in figure 5(b), while in figure 5(a) the system displays only the continuum band. We also notice that in the spectrum of figures 5(a) and (b), the continuum band appears to be very degenerated at the lower and upper edge. Unlike the case studied by Dorignac and Eilbeck [8] where they observed a continuum band in addition to two-breather bands, we do not get such a two-breather band with the initial parameter used here. However, on varying the parameters A, J, and γ we can obtain two-breather bands in addition to a continuum band. This may happen in the singular case of the $CsNiF_3$ material when it faces some physical constraints such as heating or magnetostriction that may lead to changes in its parameters and, in particular, the value of γ, as seen in figure 5(c). Henceforth, all ferromagnetic materials displaying a spin value high enough to fulfil the restriction $n \leqslant 2S$ would present an energy spectrum characterized by a single and continuum bands with a reduced gap. Their ground state is less localized. This means that the probability of finding six particles on two sites, i.e. one site with four particles and another site with two particles on an adjacent site, is weak, as shown in figure 5(d).

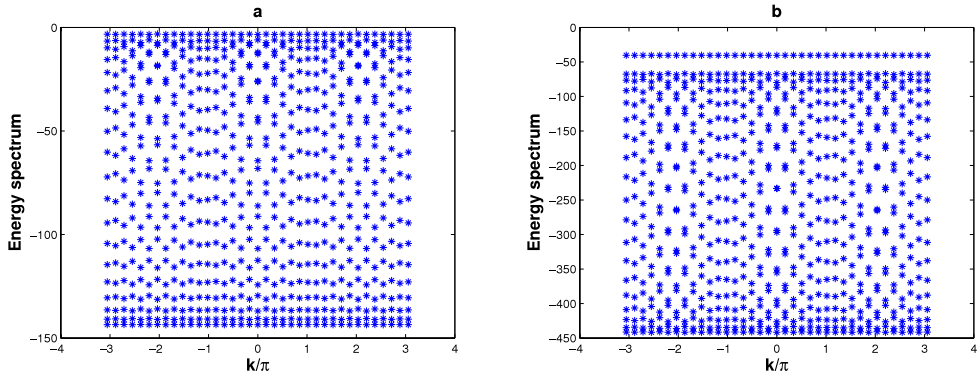

Figure 6. Detail of the energy spectrum for the Bose–Hubbard model derived from an anisotropic Heisenberg model in a periodic lattice where $n = 6$, $f = 37$, $J = 23$, and $A = 5$ corresponding to the $\{2, 4\}$ band: (a) case of repulsive nonlinearity where $\gamma = 0.17$, (b) case of repulsive nonlinearity where $\gamma = 0.085$.

The second band is the $\{2, 4\}$ band, we also obtained the Hamiltonian matrix using the same technique as in the case of $\{2, 2\}$ or $\{4, 2\}$ bands.

$$H^{(2,4)} = -\frac{2J^2}{3A\gamma}(3B + 2C)I_\sigma - \frac{BJ^2}{A\gamma}\begin{pmatrix} \Gamma & \tau & & & P^* \\ \tau^* & 0 & \tau & & \\ & \ddots & \ddots & \ddots & \\ & & \tau^* & 0 & \tau \\ P & & & \tau^* & \Gamma \end{pmatrix}, \tag{24}$$

where $P = 6e^{ik\frac{D}{B}}$, $B = (\frac{\gamma}{4} - 1)^2$, $C = (\frac{3\gamma}{4} - 1)^2$, $D = (\frac{5\gamma}{4} - 1)^2$, and $\Gamma = -\frac{1}{3B}(3B + 2C - 13D)$, I_σ is the $\sigma \times \sigma$ unity matrix. The structure of the matrix in equation (24) appears to be the same as the $\{4, 2\}$ band, the difference between the previous matrix is very small since it is similar to the two-quanta case described in [23].

The bands presented in the energy spectrum of these ferromagnetic materials appear at a first glance to be composed of flat lines where the single band can appear above the continuum for a repulsive nonlinearity, as depicted in figure 6(b) while only the continuum band appears in figure 6(a). On varying the values of A, J and γ we can obtain also the $\{4, 2\}$-like band with two-breather bands in addition to a continuum band. However, they are rather more likely than the $\{2, 4\}$ band but with a difference that this energy spectrum is rather more degenerate than the $\{4, 2\}$ case. The square wave amplitudes corresponding to the eigenvectors as a function of the position of the $\{2, 4\}$ band along the Heisenberg chain are the same as the $\{4, 2\}$ band previously presented in figure 5(d).

From a physical picture applied to the spin system, it is important to mention that there is a limitation, i.e. $n \leqslant 2S$, while the number of bosons in a pure bosonic system has no such constraint. However, there exist some materials for which the spin S is high enough so that from the spin picture the case of $n = 6$ can be seen as a process involving two adjacent spins with one being able to proceed to two switches and the other to four switches. In the case of the $CsNiF_3$ material, the process cannot happen or if it happens then the process may turn out to be more complex and the material should be under constraint since a spin can only be turned down, no more. In this framework the physical picture can be described as that of two groups of four spins and two spins adjacently situated that can be involved in one switch per group. In any case, this can be understood as the result of a local magnetization reversal process that occurs in such a ferromagnet involving only a few spins.

Using the same method as in the $\{4, 2\}$ case, the Hamiltonian matrix of the $\{3, 3\}$ band is

$$H^{(3,3)} = -\frac{3J^2B'}{A\gamma}(I_\sigma + M), \tag{25}$$

where $B' = (\frac{\gamma}{2} - 1)^2$, $M_{1,1} = \frac{1}{2} - 4\frac{D}{B'}$, $D = (\frac{5\gamma}{4} - 1)^2$, and $M_{i,j} = 0$ for any $i \neq 1$ and $j \neq 1$.

The diagonal form of the matrix in equation (25) is similar to the case of six bosons described in [8]. It is important to stress that the matrix elements in equation (25) are independent of the wavevector k. For the sake of simplicity, we have plotted the energy spectrum of this state as a function of the wavevector only for a ferromagnetic material characterized by the parameter close to those of the $CsNiF_3$ structure but with a different value of γ, as shown in figure 7(a); the eigenvalue of the corresponding $\{3, 3\}$ band appears only with two symmetric single bands.

The lower single band is in fact a result of the transformation of the continuum band into a single band. From a physical picture applied to the spin system it is once more important to re-mention that there is a limitation, i.e. $n \leqslant 2S$, while the number of bosons in a pure bosonic system has no such constraint. However, there exist some materials for which the spin S is high enough so that from the spin picture the case of $n = 6$ can be seen as two adjacent spins with each involving three switches. From our results it is clear that in the framework of six bosons for the case of other ferromagnets with spin not high enough the process should be more complex. In such a context, two groups of (three spins) a triplet can be engaged in a single switch each per group or triplet in the same time. Such a process needs experimental investigation. In any case, this can be understood as the result of a local magnetization reversal process. All ferromagnetic materials that display parameters different to those of the

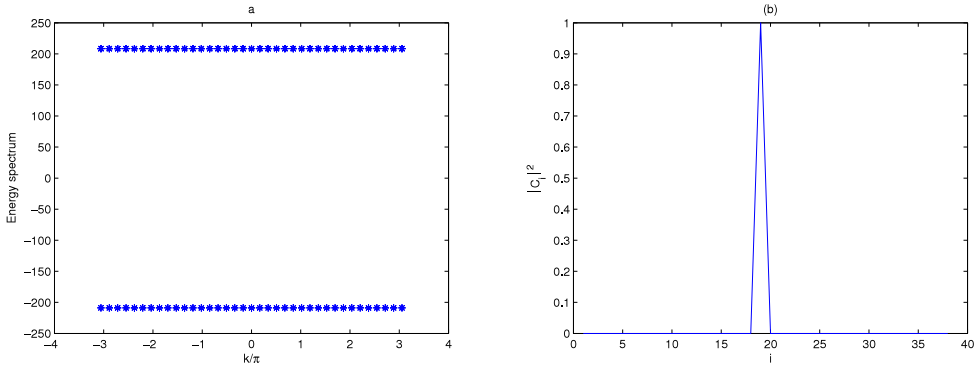

Figure 7. (a) Detail of the energy spectrum where $A = 9.5$, $n = 6$, $f = 37$, $J = 21$, and $\gamma = 0.17$; (b) square wavefunction amplitudes.

$CsNiF_3$ structure, i.e. spin value fulfilling the condition $n \leqslant 2S$ and the possibility of forming two triplet spins, have the same energy spectrum characterized by two symmetric single bands with a larger width of the gap between those single bands. Figure 7(b) shows that the ground state is mainly constituted of localized states that are located on two different positions along the chain.

6. Conclusion

This paper has been devoted to studying the detailed band structures of quantum breathers derived from a map of a quantum Heisenberg spin system in a modified Bose–Hubbard-like Hamiltonian on a periodic 1D lattice containing two, four, and six bosons. Our results confirm that when the nonlinearity is significant in the ferromagnetic materials, a single band for the localized states will split from the continuum band. Such a result has also been obtained in other nonlinear models [18–23, 26–28, 33, 39–41] for two particles and [8, 33] for four particles. From a physical picture of a ferromagnetic spin chain, the continuum band here is describing a magnetic spin chain with completely delocalized excitation along the chain whereas the case of a single band for two on-site bosons corresponds to the case of a local magnetization reversal process involving two switching spins. The results obtained for the case of $n = 4$ or 6 also show that we have succeeded from our mapping to describe the energy spectrum of a spin chain facing a local magnetization reversal process that reveals the presence of bound states through the appearance of single bands that are a signature of quantum breathers in the system. The details of the corresponding square wavefunction amplitudes of the eigenvectors as a function of the position of particles along the chain allowed us to appreciate their complex character characterized by an intrinsic localized mode. Such a Fermi–Pasta–Ulam behavior can be confirmed by the model described by the Hamiltonian given in equation (11). The anisotropy energy has the same role as the exchange integral energy, that is it can either enlarge the gap between the continuum and the localized state or order the position of the bands in the energy spectrum. An important question that may be raised is what is the localization law in real or normal mode space for the bound states so described by their energy band structure? Such an important issue will be addressed in a future paper.

Acknowledgment

One of the authors, A Kenfack-Jiotsa, acknowledges the ICTP (International Center of Theoretical Physics) of Trieste for the facilities provided.

References

[1] Eilbeck J C 2003 *Localization and Energy Transfer in Nonlinear Systems* ed L Vazquez, R S Mackay and M P Zorzano (Singapore: Word Scientific) p 177
[2] Campbell D K, Flach S and Kivshor Y S 2004 *Today* **57** 43
[3] Flach S and Gorbach A V 2008 *Phys. Rep.* **467** 1
[4] Fermi E, Pasta J and Ulam S 1955 *Los Alamos Report* No.LA-1940 (Unspecified)
in Segre E (ed) 1965 *Collected Papers of Enrico Fermi* vol II (Chicago: University of Chicago Press) pp 977–8
in Mattis D C (ed) 1993 *Many Body Problems* (Singapore: World Scientfic)
[5] Flach S, Ivanchenko M V and Kamakov O I 2006 *Phys. Rev.* E **73** 036618
[6] Ivanchenko M V, Kanakov O K, Mishangin K G and Flach S 2006 *Phys. Rev. Lett.* **97** 025505
[7] Flach S, Ivanchenko M V and Kanakov O I 2005 *Phys. Rev. Lett.* **95** 064102
[8] Dorignac J and Eilbeck J C 2004 *Phys. Rev. Lett.* **93** 025504
[9] Binder P, Abraimov D, Ustinov A V, Flach S and Zolotaryuk Y 2000 *Phys. Rev. Lett.* **84** 745
[10] Flach S and Willis C R 1998 *Phys. Rep.* **295** 181
[11] Eisenberg H S, Silberberg Y, Morandotti R, Boyd A R and Aitchison J S 1998 *Phys. Rev. Lett.* **81** 3383
[12] Elder J, Hamm P and Scott A C 2002 *Phys. Rev. Lett.* **88** 067403
[13] Xie A, Van der Meer L, Hoff W and Austin R H 2000 *Phys. Rev. Lett.* **84** 5435
[14] Alfimov G L, Konotop V V and Salerno M 2002 *Europhys. Lett.* **58** 7
Carretero-Gonz'alez R and Promislow K 2002 *Physica* A **66** 033610
[15] Lai R, Kiselev S A and Sievers A J 1997 *Phys. Rev.* B **56** 5345
[16] Pinto R A and Flach S 2007 *Europhys. Lett.* **79** 66002
[17] Tsironis G P 2003 *Chaos* **13** 657/10
[18] Nguenang J P, Pinto R A and Flach S 2007 *Phys. Rev.* B **75** 214303
Pinto R A, Nguenang J P and Flach S 2009 *Physica* D **238** 581

[19] Xin-Guang H and Tang Y 2008 *Chin. Phys. Soc.* **17** 4268-05
[20] Scott A C, Eilbeck J C and Gilhøj H 1994 *Physica* D **78** 194
[21] Scott A C, Eilbeck J C and Gilhøj H 2008 *Quantum Lattice Solitons (7 Feb.)* private communication
[22] Scott A C 2003 *Nonlinear Science* 2nd edn (New York: Oxford University)
[23] Eilbeck J C and Palmero F 2004 Quantum breathers in an attractive fermionic Hubbard model *Nonlinear Waves: Classical a Quantum Aspects* ed F Kh Abdullaev and V V Konotop (Amsterdam: Kluwer) pp 399–412
[24] Jimenez L 2006 Effects of a non-linear coupling term in both classical and quantum discrete non-linear Schrödinger equantum, Supervised by J C Eilbeck Heriot Watt University
[25] Proville L 2005 *Phys. Rev.* B **71** 104306
[26] Proville L 2005 *Phys. Rev.* B **72** 184301
[27] Eilbeck J C and Palmero F 2004 *Phys. Lett.* A **331** 201–8
[28] Pouthier V and Falvo C 2004 *Phys. Rev.* E **69** 041906
[29] Falvo C and Pouthier V 2005 *Chem. Phys.* **123** 184710
[30] Bernstein L J 1993 *Physica* D **68** 174
[31] Bernstein L, Eilbeck J C and Scott A C 1990 *Nonlinearity* **3** 293
[32] Aubry S, Flach S, Kladko K and Olbrich E 1996 *Phys. Rev. Lett.* **76** 1607
[33] Chris Eilbeck J 2003 *Proc. 3rd Conf.: Localization and Energy Transfer in Nonlinear Systems* pp 177–86
[34] Aubry S 1997 *Physica* D **103** 201
[35] Nguenang J P, Peyrard M, Kenfack A J and Kofane T C 2005 *J. Phys.: Condens. Matter* **17** 3083
[36] Gölzer B and Holz A 1987 *J. Phys. A: Math. Gen.* **20** 3327
[37] Schnalle Roman 2007 From Numerical Exact Diagonalization to spin wave theory tools to investigate magnetic molecules, University of Osnabrueck Private communication
[38] Holstein T and Primakoff H 1940 *Phys. Rev.* **58** 1098
[39] Eisenberg H S, Silberberg Y, Morandotti R, Boyd A R and Aitchison J S 1998 *Phys. Rev. Lett.* **81** 3383
[40] Eilbeck J C, Gilhøj H and Scott A C 1993 *Phys. Lett.* A **172** 229
[41] Falvo C and Pouthier V 2005 *Chem. Phys.* **123** 184709
[42] Valiejo Castañeda E 2006 *PhD Thesis: Study of Spins Order Contribution, the Charge and Structurals Effects in Double Exchange Model: Spins Ladders and Maganites* University Joseph Fourier, Grenoble I